Synergistic Weathering of Polystyrene Representative of UV and Freeze-thaw Conditions in Canadian Climates

Joel Grant
Department of Chemical Engineering
McGill University, Montreal
December 2021

A thesis submitted to McGill University in partial fulfillment of the requirements of the degree of
Master of Engineering in Chemical Engineering

Table of Contents

Abstract

Plastic pollution in aquatic and terrestrial environments is a growing global concern. While the identification of macro- and micro-plastics in outdoor samples has been well-documented in recent years, observing and characterizing nanoplastic formation remains a challenge. This is largely due to the presence of naturally occurring organic particulate matter and other contaminants when samples are collected from the natural environment. Thus, studies of plastic weathering under controlled conditions are of interest to investigate plastic fragmentation and degradation. This provides the opportunity to consider synergistic weathering with ultraviolet (UV) irradiation exposure followed by freeze-thaw cycling such as that observed in the climate of southern Quebec.

This thesis details the effects of weathering on polystyrene sheets by investigating changes in bulk mechanical properties, surface roughness variations, and particle release. Polystyrene was chosen because it is frequently found in aquatic environments as a result of inappropriate disposal. Weathering polystyrene sheets via 18-weeks of UV exposure followed by fourteen 24-hr cycles of freeze-thaw in filtered reverse-osmosis water led to increases in bulk and surface hardness of the polystyrene. The storage modulus curve of weathered polystyrene underwent a shift and increase in glass transition temperature. This showed a change in stiffness and embrittlement of the surface layer due to the formation of crystallites and oxidation. Surface roughness measurements also increased because of erosion of the core surface. Particles released into the leachate were analyzed by Scanning Electron Microscopy and Nanoparticle Tracking Analysis. It was found that micron-sized and submicron-sized particles were released upon weathering of the plastic. Films of the particles were confirmed to be polystyrene with Fourier Transform Infrared Spectroscopy. These

data suggest that seasonal variations may be associated with increased release of polystyrene particles from the bulk plastic.

Résumé

La pollution plastique dans les environnements aquatiques et terrestres est une préoccupation mondiale croissante. Alors que l'identification des macro- et microplastiques à partir d'échantillons extérieurs a été bien documentée ces dernières années, l'observation et la caractérisation de la formation des nanoplastiques reste un défi. Cela est dû en grande partie à la présence de particules naturelles et d'autres contaminants lorsque les échantillons sont collectés dans l'environnement naturel. Par conséquent, les études de l'altération des plastiques dans des conditions contrôlées sont utiles pour étudier la fragmentation et la dégradation des plastiques. Ceci permet de considérer l'altération synergique avec une exposition aux ultraviolets (UV) suivie d'un cycle de gel-dégel tel qu'observé dans le climat du sud du Québec.

Cette thèse détaille les effets de l'altération sur les feuilles de polystyrène en étudiant les changements des propriétés mécaniques, les variations de la rugosité de surface et la libération de particules. Le polystyrène a été choisi parce qu'il est fréquemment retrouvé dans les environnements aquatiques lors d'une élimination inappropriée. L'altération des feuilles de polystyrène pendant 18 semaines d'exposition aux UV, suivie de quatorze cycles de 24 heures de gel-dégel dans de l'eau filtrée par osmose inverse, a entraîné une augmentation de la dureté de la masse et de la surface. La courbe du module de stockage du polystyrène altéré a subi un déplacement et une augmentation de la température de transition vitreuse. Cela a montré un changement de la rigidité et une fragilisation de la couche de surface due à la formation de cristallites et à l'oxydation. Les mesures de la rugosité de surface de la hauteur de pic réduite ont également augmenté en raison de l'érosion de la surface du noyau. Les particules libérées dans le lixiviat ont été analysées par microscopie électronique à balayage et analyse de suivi des

nanoparticules. Il a été démontré que des particules microniques et submicroniques ont été libérées par les conditions météorologiques. Les films des particules ont été confirmés comme étant du polystyrène par spectroscopie infrarouge à transformée de Fourier. Ces données suggèrent que les variations saisonnières peuvent être associées à une libération accrue de polystyrène.

Acknowledgements

I am very grateful for the support I received during my Master’s thesis. There were many individuals who contributed and worked collaboratively to make this possible. I would like to thank my supervisor, Prof. Nathalie Tufenkji. I really appreciated her mentorship throughout my graduate studies. Dr. Laura Hernandez and Dr. Jeffrey Farner were instrumental in their efforts in meeting with me on a weekly basis. Prof. Richard Chromik and Dr. Sima Ahmed Ali Dokht helped me tremendously when learning about surface roughness and mechanical properties tests. I thank them for their generosity and incredible knowledge. Thank you to Prof. Pascal Hubert and Lucie Riffard for allowing me the opportunity to conduct DMA experiments and for teaching so openly in their spare time. I am grateful for Dr. Parvin Shakerifard for helping me with the long and tedious task of drop casting films. Sara Matthews was very supportive in that she assisted me on the CytoViva for my research project course. She also was a strong supporter of the 2019 Canadian Indigenous Science and Engineering Society Conference hosted at McGill. Thank you to everyone in the Biocolloids and Surfaces Laboratory. Learning about everyone’s research during group meetings was a pleasure. Thank you everyone who assisted me in conducting freeze-thaw experiments.

It is with great pleasure that I would like to thank McGill University Financial Aid, specifically Cara Piperni for her efforts in facilitating my funding as an Indigenous student. I am particularly fortunate to have received funding from the Rathlyn Fellowship, NIB Trust Fund, Indspire, Grad Excellence Award, Meighen Bursary, PGSS Bursary and the American Indian Science and Engineering Society. I would also like to thank my own Nation, the Métis Nation of Alberta (Region 3, Treaty 7 territory) for Band funding from the Rupertsland Institute. I am appreciative

of the community support I received from the First Peoples' House and the Medicine Bear Singers. I am thankful for the opportunity of being a senior camp councillor with the Eagle Spirit Science Futures Camp for Indigenous youth. Kinanâskomitin.

Contribution of Authors

The manuscript-based format was selected for this thesis. It is in accordance with the guidelines provided by McGill University. There are four primary chapters: Chapter 1 introduces the thesis to the reader; Chapter 2 highlights the literature and research objectives; Chapter 3 is the manuscript; and Chapter 4 comprises a conclusion and future recommendations.

The manuscript titled, “Effects of Weathering and Freeze-thaw Representative of Canadian Climates on Degradation of Polystyrene” is authored by Joel Grant, Laura Hernandez, Jeffrey Farner, Richard Chromik and Nathalie Tufenkji. Experimental design, data collection, instrumentation, analysis and writing the manuscript was a collaborative effort. Joel Grant set-up the experiments and conducted sampling for mechanical properties tests and surface roughness. Joel characterized the bulk polystyrene samples and prepared films of the leachate for Laura Hernandez, who characterized the release of particles with SEM, NTA and FTIR measurements. Laura Hernandez assisted with revising the manuscript along with Jeffrey Farner, Richard Chromik and Nathalie Tufenkji. Jeffrey Farner facilitated experimental design, statistical analysis and data representation. Nathalie Tufenkji and Richard Chromik provided guidance in experimental design, data interpretation, and revised the manuscript.

1 Introduction

The rate at which plastic pollution is accumulating in terrestrial environments is alarming. Although there have been concerted efforts to reduce plastic consumption, it just isn’t enough to solve this prevailing global issue. According to Borrelle et al. the persistent amount of plastic debris accumulating in the environment is far outweighing efforts to mitigate plastic production [1]. Imposed legislation and initiatives will not be sufficient to minimize the impact of plastic pollution for at least the next decade [2]. Furthermore, there is the threat of bulk plastics in the environment undergoing weathering that leads to fragmentation. The release of smaller fragments is identified as microplastics or nanoplastics and has been reported to have unfavorable effects [3-5].

The U.S. Environmental Protection Agency categorizes plastics that are 0.1 - 5 mm in size as microplastics [6]. The detection of microplastics has been studied thoroughly [7-16], but environmental concentrations of nanoplastics are challenging to determine because of their small size and the higher likelihood of acquiring contaminants when sampling [17]. Nanoplastics are defined in the range of 1 nm up to 1,000 nm according to the US National Nanotechnology Initiative [4]. Literature has many inconsistencies with some studies citing up to ~ <1 um in size [4, 6]. Nonetheless, nanoplastics are transported to the aquatic environment either as primary or secondary nanoplastics [6]. This study focuses on the weathering of plastic sheets and the subsequent release of secondary nanoplastics derived from the fragmentation and degradation of bulk polystyrene.

Weathering of bulk plastics induces several degradation processes leading to the release of micro- and nano-plastics into the environment [2]. These processes include photooxidation, hydrolysis, chemical oxidation, and physical abrasion [18-21]. Plastics will be subjected to these weathering processes synergistically. This is a limitation for many studies that examine microplastic weathering in the laboratory setting, whereby they focus on isolating one degradation mechanism [2]. Accelerated weathering systems simulate degradation processes over a shorter period of time and the obtained information is extrapolated to real world conditions. This is not always realistic and or an accurate portrayal of the actual effects of weathering on plastics in outdoor environments. However, this study aims to simulate synergistic weathering conditions of UV irradiation followed by freeze-thaw to illustrate the effects of seasonal variations in the southern Quebec region. Global solar UV exposure is reported to have a mean of 12.23 W/m^2 with the highest monthly average of 33.49 W/m^2 (July) and lowest monthly average of 3.53 W/m^2 (December) [22]. Weathering chamber conditions (23 W/m^2) were selected to mimic natural UV exposure within the seasonal temperature profile relevant to a colder climate region. Upper layers of ground soil in southern Quebec experience a temperature range of approximately -10 ºC to +10 ºC [23, 24]. However, during colder months such as December, temperatures can reach as low as -20 ºC due to subarctic-like freezing conditions [25]. Cycles of freeze-thaw were carried out between –20 ºC and +4 ºC to overlap with real world conditions. These environmental conditions illustrate a temperature profile within Canada’s winter shoulder periods of interest [26, 27]. Our closed system weathering has the benefits of no contamination; this allows for optimal characterization of bulk polystyrene degraded samples and the subsequent release of micro- and nanoplastics. The findings have enabled us to demonstrate a better understanding of the fragmentation process in unique environmental conditions.

The overall objective of this research is to establish whether bulk polystyrene releases micro- and nanoplastics as a result of exposure to UV irradiation followed by freeze-thaw in a closed system. No previous published studies have examined the formation of microplastics and nanoplastics in a controlled environment from UV-FT synergistic weathering. The following objectives outline the goals of the research:

- Evaluate the effect of a simulated Canadian weathering condition on the release of polystyrene microplastics and nanoplastics. Simulate freeze-thaw cycling conditions in a model laboratory weathering system. Design a freeze-thaw cycling experiment with repeatability. Implement synergistic weathering of UV irradiation followed by freeze-thaw to better mimic the seasonal variations of the southern Quebec region.

- Characterize the chemical composition, size and morphology of micron and submicron particles in the leachate wherein weathered sheets of polystyrene were placed. Assess nanoplastic concentration.

- Compare the mechanical properties of bulk plastics before and after degradation. Identify a connection between bulk surface property changes and fragmentation of particles. This is achieved by examining hardness, modulus, and surface roughness.

- Compare the quantification and characterization of microplastics and nanoplastics to literature findings. Polystyrene was chosen for this reason – it has been well documented, studied and is one of the primary plastics of environmental concern.

2 Background

2.1 Outdoor Weathering and Challenges with Simulated Weathering

Outdoor weathering experiments primarily focus on various microplastic release or the determination of a product life cycle of a bulk plastic via ASTM Standard D1435 [28]. This standard is designed to test the outdoor weatherability and durability of materials with relation to mechanical function. When evaluating the effects of weathering on plastic both in the outdoor environment and in the simulated laboratory setting, there is a lack of protocol harmonization [2]. Studies have focused their attention on isolating certain degradation mechanisms such as photooxidation, hydrolysis, biodegradation, and mechanical stress [6, 19, 29, 30]. Currently, there are very few studies examining outdoor weathering in a seasonal climate, whereby UV exposure and freeze-thaw prevalently takes place.

2.2 Selection of Polystyrene as Polymer of Interest

Polystyrene can be found in abundance outside, subjected to the natural environment due to improper discard. The chemical composition of polystyrene is $(C_8H_8)_n$ as it is a hydrocarbon polymer consisting of styrene monomers; therefore, it is a polymer of choice for weathering experiments because it is easily identified with characterization techniques such as Fourier Transform Infrared (FTIR) Spectroscopy, Raman Spectroscopy, and Nuclear Magnetic Resonance Spectroscopy [2].

2.3 Simulated Weathering of Canadian Climate – Southern Quebec Region

Canada provides an environment with four distinct seasons that illustrate the diverse effects of outdoor weathering on microplastic and nanoplastic formation. The southern Quebec region provides a unique opportunity to simulate UV exposure followed by freeze-thaw cycling in the laboratory setting. As southern Quebec climate conditions have yet to be examined with regard to the effects on nanoplastic quantification and identification, conducting a simulated weathering experiment to mimic freeze-thaw cycling will enable a new type of assessment. In addition, there are several terrestrial environments around the world. These climates fluctuate seasonally with similar weathering conditions that have been overlooked.

2.4 UV Weathering Effects on Polymers

It is important to understand the reported effects of UV weathering on plastics. Cai et al. tested three different plastic polymers (polypropylene, polyethylene and polystyrene) in pristine condition and exposed them to UV irradiation in seawater, in ultrapure water and in the air for a period of three months [19]. The effects of UV exposure were evaluated using FTIR. It was found that absorption peaks around 3300 cm^{-1} and 1712 cm^{-1} appeared more prominent with increased exposure time for the air, ultrapure water and simulated seawater conditions [19]. It was concluded that weathering led to the formation of hydroxyl groups and carbonyl groups [19]. Scanning electron microscopy of the weathered polymer surfaces showed cracking, flakes and granular oxidation [19]. Cai et al. concluded that plastics undergoing UV exposure become more brittle [19]. There was also an increase in cracks and flakes on the surface that lead to higher fragmentation of microplastics and nanoplastics [19].

Gewert et al. provides an overview of degradation pathways for polymers floating in the marine environment [31]. Plastics like polyethylene, polypropylene and polystyrene have a carbon backbone and therefore, are more susceptible to photo initiated oxidative degradation [31]. Figure 1 displays the degradation pathways associated with UV exposure for these plastics. For polystyrene, when subjected to UV irradiation, its phenyl ring gets excited causing energy to be transferred to the closest C-H bond [31]. Cleavage of the hydrogen is initiated, and a polymer free radical is formed. This results in lower molecular weight, carbonyl group formation, chain scission and crystallites within the amorphous structure of polystyrene [31, 32]. All these well documented findings of the effects of UV on bulk polymers provide a better understanding of evaluating mechanical properties, surface roughness and the fragmentation of particles in our characterization research.

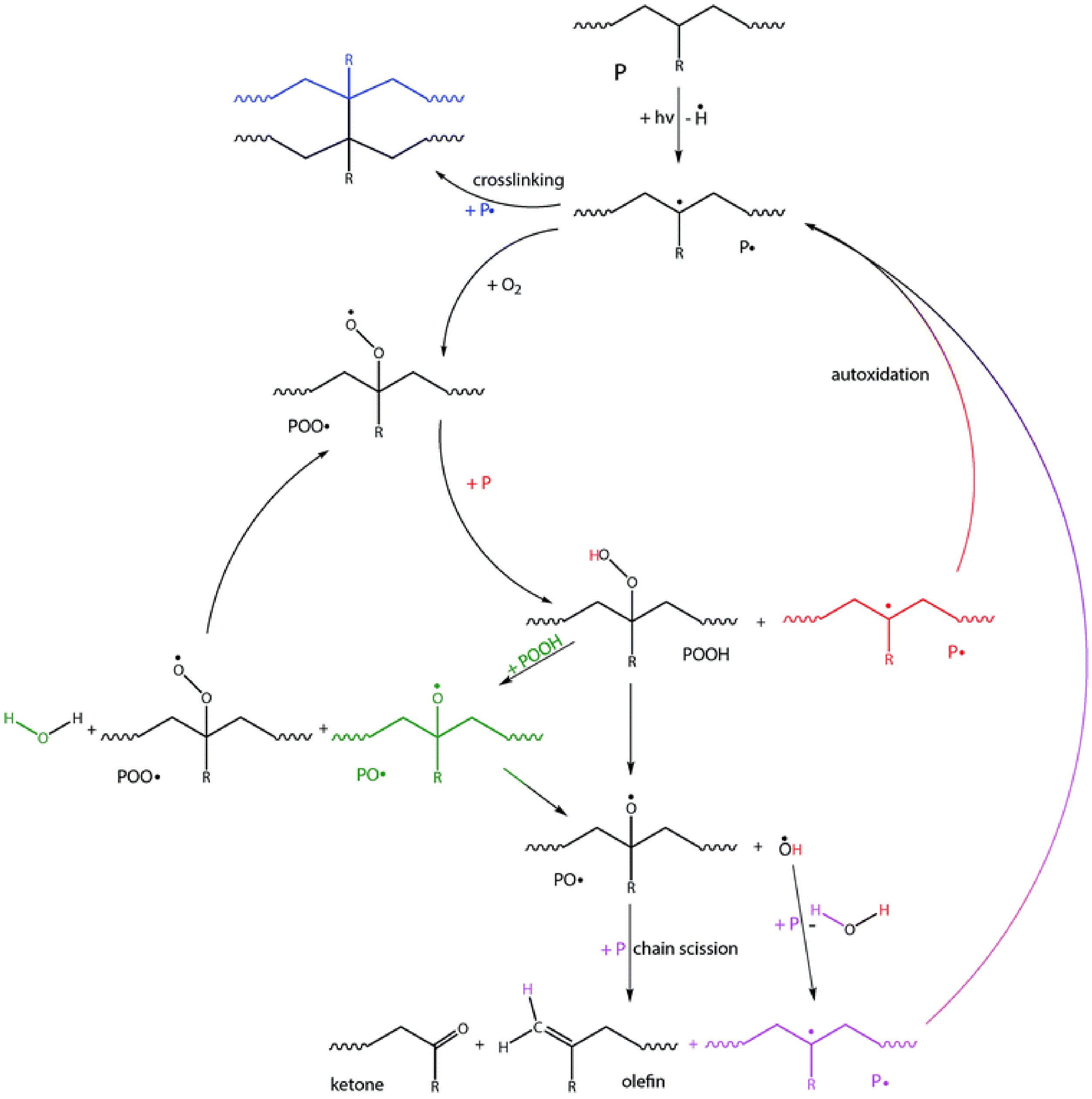

Figure 1. *Degradation pathways illustrated for polyethylene (R = H), polypropylene (R = CH_3) and polystyrene (R = aromatic ring). P is shown as the polymer backbone where initial photolytic cleavage of C–H bond on the polymer backbone occurs [31].*

2.5 Freeze-thaw Weathering

Freeze-thaw cycling experiments can be implemented as a model laboratory weathering system. Adhikary et al. investigated the durability of wood-plastic composites by subjecting them to freeze-thaw cycling [33]. The samples contained polypropylene and high-density polypropylene. It was found that flexural strength and stiffness decreased with freeze-thaw weathering [33]. However, SEM analysis depicted fractural bonding at the surface of the bulk composites [33]. This may indicate the result of microplastic and nanoplastic fragmentation.

The performance of extruded polystyrene board was analyzed by Niu et al. by subjecting samples to hundreds of freeze-thaw cycles [34]. Young's modulus and creep strain decreased significantly [34]. This may indicate that the mechanical properties of polystyrene in our study will decrease due to the axial forces of compression occurring on the surface from continued ice crystallization and melting.

Nanoparticles may form aggregates when subjected to freeze-thaw conditions. Farner et al. exhibited an increase in nanoparticle aggregation upon freeze-thaw cycling of titanium dioxide suspensions [35]. It was determined that nanoparticles formed heterogeneous aggregate sizes after a single freeze-thaw cycle [35]. Furthermore, stresses induced by freeze-thaw allowed for organics to be removed from the surface of nanoparticles, facilitating aggregation [35]. More polymer studies are needed in the determination of mechanical property changes and nanoplastic release upon freeze-thaw exposure. Thus, this study begins to address this knowledge gap.

3 Effects of Weathering and Freeze-thaw Representative of Canadian Climates on Degradation of Polystyrene

Abstract

There is a need to evaluate the effects of synergistic weathering processes on plastics to compare real outdoor environments with the efficacy of simulated indoor conditions. Several studies utilize controlled weathering protocols to focus on isolating primary degradation processes like photooxidation, biodegradation, and mechanical degradation. This is beneficial to better understand such degradation mechanisms at work, along with the ability to identify polymer chemical compositions due to the removal of potential contaminants that would otherwise be present from outdoor sampling. However, complex weathering conditions arise in many overlooked climates of interest, whereby plastics accumulate at an alarming rate. One such climate is the southern Quebec region in Canada. Canada has fluctuating seasons that undergo conditions of prolonged UV irradiation exposure as well as freezing and thawing. In this work, we illustrate that a closed system experiment of 18-weeks of UV irradiation followed by 14-cycles of freeze-thaw weathering (UV-FT) on polystyrene led to the release of microplastics and nanoplastics. Characterization of weathered bulk polystyrene yielded changes in mechanical properties and surface roughness. Our findings illustrate that the synergistic effects of UV-FT enabled embrittlement, oxidation and particle fragmentation on the surface layer. Combined weathering degradation processes in a closed system needs to be further investigated with added complexity, as many climates throughout the world have similar conditions, especially with regard to freeze-thaw weathering. We believe our study acknowledges this gap in current research.

3.1 Introduction

Despite their beneficial applications and the economic advantages associated with their use, plastics present a global environmental issue. In 2017, the global production of plastics was 320 million tonnes (Mt) per year [36]. It is estimated that by 2025 at least 250 Mt of waste plastic will have accumulated in the natural environment as a result of pollution and mismanagement [37]. This plastic pollution exists at multiple sizes: macro-, micro- and nanoplastics. Microplastics are ~ 0.1 - 5 mm in size, while particles larger than 5 mm are commonly referred to as falling within the macro-scale [6]. While size alone cannot be used to meaningfully define nanoplastics [6], this smallest fraction of particles is typically on the order of ~0.5 µm in size.

Plastic in the environment may be considered either primary or secondary plastics [6]. For example, primary plastics include microplastics and nanoplastics present as additives in both personal and commercial based products, whereas, secondary plastics are derived from the fragmentation and degradation resulting from, e.g., the outdoor weathering of primary plastics [38-41]. While the presence of macro- and microplastics is well documented [7-16], current sampling and detection techniques have not been able to provide conclusive data on environmental nanoplastic concentrations [17]. This is largely in part because of the abundance of organic matter in samples collected from the natural environment [42]. Therefore, simulated laboratory weathering whereby conditions can be controlled within a closed system enable nanoplastics to be detected more readily [43].

The degradation of bulk macroscopic plastics to microplastics is evidence of a degradation process that can result in further nano-size fragmentation of plastics [17]. The degradation of plastics can occur by a variety of processes including hydrolysis, photo-oxidation due to UV exposure, mechanical abrasion by sand or wave action, and biodegradation [17]. Some of these processes work synergistically. A review of the literature on the environmental weathering of plastics reveals that changes in the mechanical properties and surface roughness of bulk plastics upon weathering are generally overlooked. Although the American Society for Testing and Materials (ASTM) mechanical property standards on plastics are primarily used to determine a material's durability, there remains an opportunity to utilize these tests to better understand the effects of weathering on both the bulk and surface properties of a plastic. Mechanical property changes may provide insight as to the fractionation process of micro- and nanosized particles from bulk plastic surfaces.

The weathering of polystyrene was examined in this study because of its widespread use in various applications such as outdoor products (e.g., garden furniture, children's toys), and building materials [44]. Polystyrene is frequently found in marine environments upon material discard [45]. Its chemical composition features polymerized styrene monomers that can easily be detected using characterization techniques such as Fourier Transform Infrared (FTIR) spectroscopy [46]. Ward et al. demonstrated that polystyrene degrades quickly when subjected to natural sunlight [47]. In addition to UV exposure, the Canadian environment provides four distinct seasons that can impact rates of plastic degradation. In particular, cold temperatures and freeze-thaw cycling are characteristic of the southern Quebec region. Previous work examining the release of metal oxide nanoparticles from painted or stained surfaces exposed to natural and laboratory induced freeze-thaw cycling has demonstrated the enhanced release in the presence of temperature variations [48, 49]. Additionally, Adhikary et al. investigated the durability of wood-plastic composites containing polypropylene and high density polyethylene by subjecting them to freeze-thaw cycling, observing that flexural strength and stiffness decreased with freeze-thaw weathering [33]. Moreover, Scanning Electron Microscopy (SEM) analysis depicted fractural bonding at the surface of the bulk composites [33], possibly indicating microplastic and nanoplastic fractionation sites.

This controlled laboratory study investigates the formation of secondary nanoplastics resulting from the weathering of bulk polystyrene sheets. We compare the degradation behavior of polystyrene when exposed to two weathering factors, UV exposure and freeze-thaw cycling, conducted to mimic a Canadian climate (or Northern climate). We hypothesized that the combination of UV and freeze-thaw treatments would lead to greater weathering and particle release than either treatment alone. The study also examines the effects of these weathering treatments synergistically just as this will occur in an outdoor environment.

3.2 Materials and Methods

*3.**2.1 Preparation and Weathering of Polystyrene Sheets***

Polystyrene sheets (4 ft x 4 ft from McMaster-Carr) were cut into coupons of 7 cm x 15 cm with 1.59 mm thickness using clean stainless-steel scissors. A biological safety cabinet dedicated to plastic work and a cotton lab coat were used at all times when handling samples. The cut polystyrene coupons were rinsed three times with 0.1 µm filtered RO water, and dried in a desiccator before use. Plastic sheets were weathered via 3 treatments: (i) UV exposure alone (UV), (ii) UV followed by freeze/thaw (UV-FT), or (iii) freeze/thaw exposure alone (FT).

For UV exposure, polystyrene coupons were placed between two clean glass sheets within a UV-weathering chamber (dimensions 2 ft x 2ft x 1ft). A total of 10 bulbs were placed above the glass sheets and an additional 10 bulbs were placed below the glass sheets to ensure coverage from all angles. The bulbs were purchased from the light manufacturer EiKO (8W Black Light Blue UV-A T-5 G5 Base, UV-A 365 nm). Polystyrene coupons were subjected to 18-weeks of UV-exposure at room temperature with an average measured UV-light irradiance of 23 W/m^2 (measured with the UV Radiation Apogee MU-200 serial #1237 irradiance meter). The position of the coupons within the chamber was rotated every six weeks to ensure an equal distribution of UV exposure.

For FT exposure, polystyrene coupons were kept in the dark for 18 weeks between two glass sheets, following the same procedure as UV exposure, above. After this initial period, the polystyrene coupons were placed inside 1 L glass jars that had been previously cleaned in the biological safety cabinet with an acetone rinse (10%), ethanol rinse (15%) and then 0.1 µm filtered RO water rinse. Next, 250 mL of filtered RO water was added to each glass jar along with a polystyrene coupon. Triplicates of each sample and one procedural blank sample (only filtered RO water) were made for the following treatments: control (18-weeks in the dark followed by 14-cycles in the fridge at 4 ^{o}C), UV-FT (18-weeks of UV-exposure followed by 14-cycles of freeze-thaw), and FT (18-weeks in the dark followed by 14-cycles of freeze-thaw). One freeze-thaw cycle was 12 hrs in a freezer at -20 ^{o}C followed by 12 hrs in a fridge at 4 ^{o}C. Upon the completion of each treatment, coupons were retrieved for bulk property analysis. The 250 mL of water in each glass jar is referred to as the leachate from the polystyrene coupons.

3.2.2 Laser Cutting

Treated polystyrene coupons were perforated using a CM1290 laser cutter by SignCut Inc. with the cutting parameters set to 34 for the power and 20 for the speed. Coupons were laser cut into squares with an area of 25 mm^2 for Rockwell hardness, microhardness and surface roughness measurements. The sample dimensions were determined in accordance with a modified (where sample thickness = 1.59 mm) ASTM D785 standard for the Rockwell hardness testing of plastics [50]. Strips of polystyrene were also laser cut from each coupon with an area of 35 mm x 10 mm for Dynamic Mechanical Analysis. An AutoCAD file was sourced to specify the desired cutting dimensions for all of the polystyrene coupons. This ensured an even cut with minimal damage being introduced to the sample edges. All test specimens were cut from the section of polystyrene that was submerged in water (when applicable).

3.2.3 Bulk Plastic Properties

3.2.3.1 Rockwell hardness

Bulk property hardness was analyzed using the Mitutoyo HR-500 Rockwell Hardness Tester with ASTMD75. The HRR 60 scale was selected for plastics with the Suntec Corp. HRRW ASTM hardness standard. Calibration was performed before each test to ensure that a 115.2 hardness value was obtained within a ± 5% acceptable error. Indentations were completed at 60 kgf with a 1/2" diameter steel ball. Low speed was used with a timer of 5 sec per indentation. Five measurements were taken on each of three coupons to obtain a total of 15 measurements per treatment. Subsequent indents were performed with adequate spacing.

3.2.3.2 Microhardness

A Clark CM100 AT Vickers microhardness instrument was used to indent the surface of the treated polystyrene square coupons. Indentation was performed with a diamond head indenter. The indentation load was set to 10 gf with a speed of 10 sec. Five indentations were conducted on each of three coupons to obtain a total of 15 measurements for each treatment. The computer software, Clemex CMT was utilized to generate indentation images from the built-in camera. This was completed at an optical threshold of 500x with the CM 100 AT M50/0.68 magnification setting. To obtain the Vickers Hardness (Hv) value, the applied force is divided by the surface area of the indentation.

3.2.3.3 Dynamic Mechanical Analysis

Mechanical properties such as the Storage Modulus, *E'* Loss Modulus, *E''* and glass transition temperature, T_g were obtained using TA Instrument's Q800 Dynamic Mechanical Analyzer. The instrument was calibrated with a stainless-steel rectangle (length: 35 mm, width: 10.33 mm, thickness: 2.37 mm) and treated polystyrene strips were placed in the Dual Cantilever (Flexure) clamp. Triplicate strips of each treatment were measured within a vacuum chamber with a final temperature of 180 ^{o}C, a frequency maintained at 1 Hz and an amplitude of 50 µm. The amplitude was determined from the linear viscoelasticity region at 1 Hz and 25^{o}C. The testing mode was set to DMA Multi-Frequency-Strain with a Temperature Ramp/Frequency Sweep at 6 ^{o}C/min.

3.2.4 Surface Roughness

Local areal scans of the treated 25 mm^2 polystyrene laser cut square samples were performed with a Zygo 3D optical surface profiler. Mx Software was utilized to determine the surface roughness parameters S_a and S_{pk} at 20x, 50x and 100x magnifications. S_a is the average roughness defined by measuring the difference in height of each local maximum point compared to the arithmetic mean. Conversely, S_{pk} highlights the mean value of the local height relative to the core surface. Three measurements at random surface locations were taken on three separate square coupons per treatment, for a total of N = 9 per treatment. The scan length was set to 20 µm with auto focus/tilt and the Coherence Scanning Interferometry setting.

3.2.5. Characterization of Leachate from Polystyrene Weathering

3.2.5.1 Analysis of Leachate Using Scanning Electron Microscopy and Nanoparticle Tracking Analysis

Leachates for each coupon and the procedural blank (filtered RO water only) were analyzed in triplicate to corroborate the presence of particles using SEM and nanoparticle tracking analysis (NTA). All sample preparation for SEM was performed in a biosafety cabinet with laminar flow. To prepare the samples for SEM, a hydrophilic polycarbonate membrane filter (Sterlitech # PCT00147100, pore size 10 nm) was attached to an SEM stub (Ted Pella #16084-1) using carbon tape (Ted Pella #16111). Subsequently, 2 mL of the leachate were deposited on the filter, 10 µL at a time. The samples were allowed to dry in the biological safety cabinet. After the total volume was deposited and dried, the filters were coated with a 2 nm layer of platinum (Leica Microsystems EM ACE600 Sputter Coater) and subsequently observed with SEM (FEI Quanta 450 environmental SEM, 5 kV, spot size: 3.0). Fifteen images were taken randomly on each of three samples at both low (500×) and high (30,000×) magnification. This yielded 45 images at each magnification per treatment.

The concentration of particles smaller than ~1 µm was estimated using NTA (LM14 instrument with 532 nm green laser, NanoSight Ltd.). Briefly, 1 mL of leachate from each triplicate was introduced into the NTA chamber and particles were tracked for 60 sec (335 shutter aperture, 0-5 gain). After tracking more than 200 particles, the NanoSight software was used to calculate the number concentration of particles. Each triplicate was measured three times, for a total of nine measurements per treatment. The NTA chamber was emptied and cleaned in between each measurement. The chamber was cleaned by using a Kimwipe with type I water followed by acetone, and ethanol.

3.2.5.2 Characterization of the Leachate using FTIR Spectroscopy

The leachate was separated into micro-sized (> 1.5 µm) and submicron sized (< 1.5 µm) fractions using a glass fiber filter. A volume of 50 mL of leachate was filtered through a glass fiber filter (Fisher 934-AH #09-870A) that was held on a stainless-steel filter holder (Sterlitech #301200). The filtrate was collected and contained the particles < 1.5 µm in size. The filter was then carefully flipped and subsequently backflushed using 50 mL of LC-MS grade water (Fisher #W64). This fraction collected contained the particles > 1.5 µm. A volume of 22 mL of each fraction was then separately drop-cast onto aluminum foil. This volume was achieved by adding one droplet (0.5 mL) of leachate and letting it dry in order to minimize the area in which the film of particles would form.

Unweathered polystyrene, weathered polystyrene, and both micro-sized and submicron-sized particle films were characterized using a Spectrum TWO Fourier Transform Infrared Spectrometer (FTIR) with a single-bounce diamond (PerkinElmer) in attenuated total reflection mode (ATR). The spectra were taken from 500 to 4,000 cm^{-1}, and 16 scans were performed. There was no visible film formed when drop-casting the procedural controls; nonetheless, the surface was analyzed with FTIR to corroborate the absence of polystyrene.

3.3 Results and Discussion

3.3.1 Effects of Weathering on Polystyrene Bulk Mechanical Properties

The degradation of material mechanical properties can be evaluated by examining hardness, which measures the surface’s resistance to deformation [50]. Hardness can be determined at both the macro-scale and the micro-scale. An increase in polymer hardness is indicative of embrittlement and physical ageing [51].

The Rockwell R scale measures bulk macro hardness. Following ASTM D785 [52], exposure to UV-FT (80.5 ± 2.54, average ± standard deviation) and UV (77.8 ± 2.08) treatments resulted in significant increases ($p < 0.05$) in Rockwell hardness as shown in Figure 2. Exposing polystyrene to FT cycling after UV treatment resulted in greater Rockwell hardness values than UV alone. In comparison, no significant differences were observed in the average Rockwell hardness numbers for control, unweathered, and FT samples (69.1 ± 3.38, 69.4 ± 4.78, 67.5 ± 6.83, respectively). These results suggest that UV exposure is necessary for changes to the bulk material properties and that weathering processes such as freezing temperatures can act synergistically.

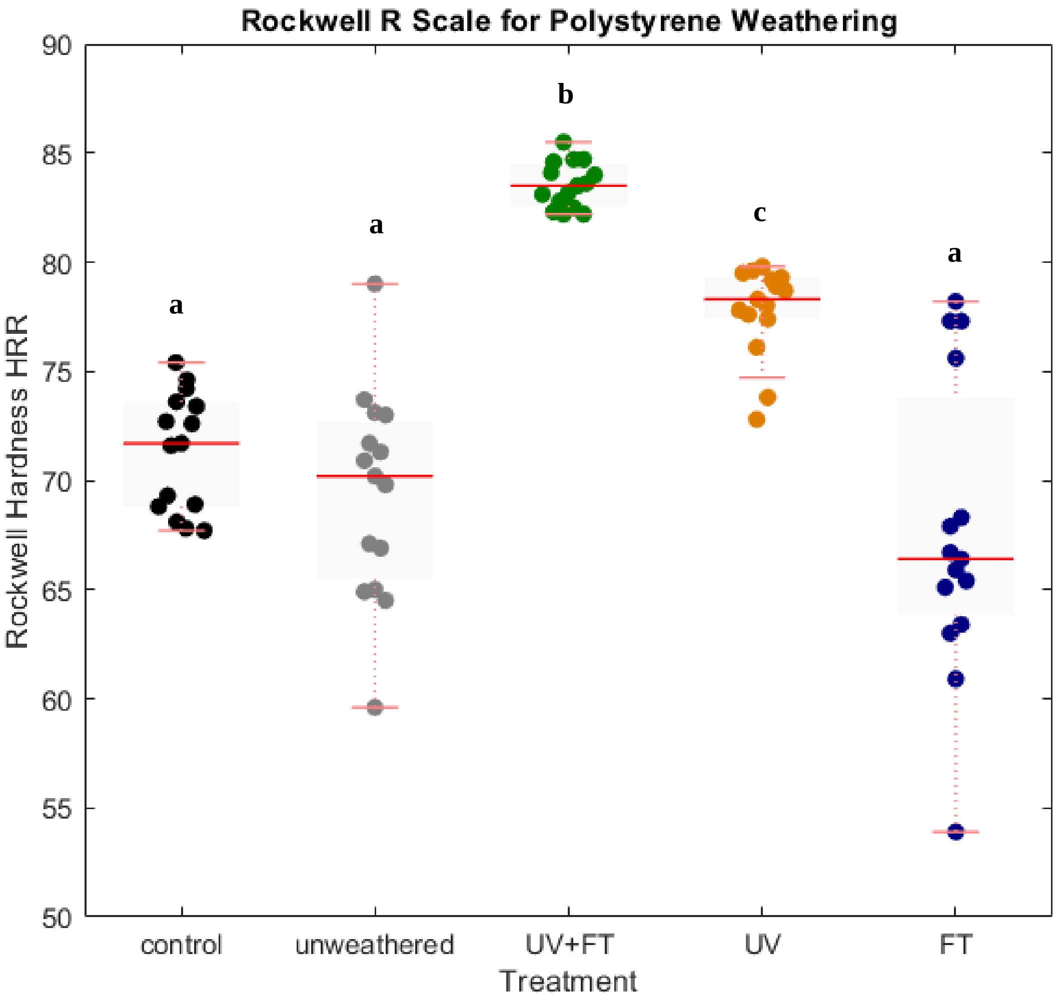

Figure 2. *Rockwell hardness results where N = 15 measurements for each treatment. Letters denote results of a 1-way ANOVA test performed with post hoc Tukey's HSD (p < 0.05). The central line for each plot represents the median. The bottom and top edges of the box indicate the 25th and 75th percentile, respectively. Whiskers extend to the most extreme data points not considered outliers.*

Microhardness Vickers characterization identifies hardness at the micro-scale [53]. Figure 3 illustrates the significant increase in Vickers hardness for UV-FT (20 ± 0.93 Hv) and UV (16 ± 0.56 Hv) treatments when compared to the control and unweathered coupons. Conversely, FT (8.7

± 0.62 Hv) resulted in a significant decrease in microhardness compared to both control and unweathered treatments (10 ± 0.59 Hv and 9.9 ± 1.0 Hv, respectively). This decrease in hardness observed for FT samples at the micro-scale was not significant at the macro-scale (c.f. Figure 2).

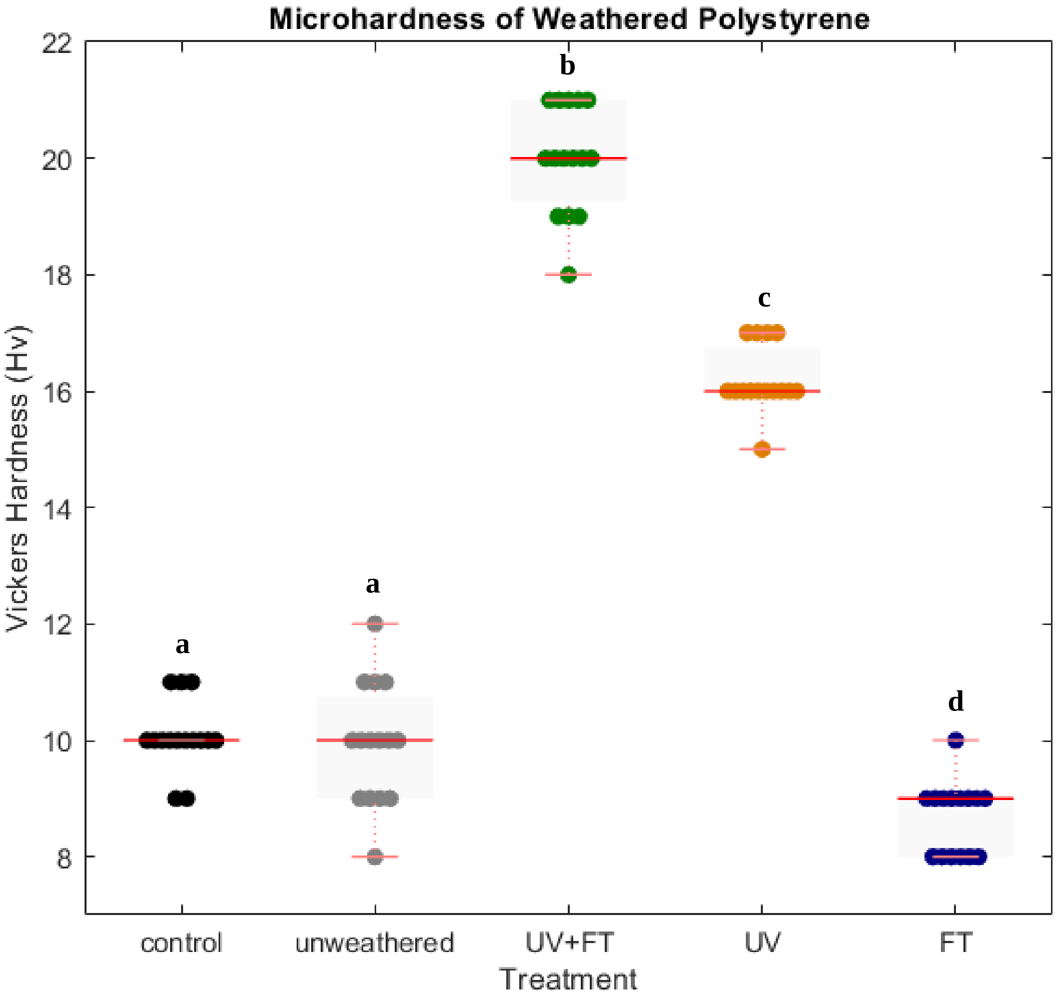

Figure 3. *Microhardness box plot results depicting a 1-way ANOVA test performed with post hoc Tukey's HSD ($p < 0.05$). A total of 15 measurements were taken per treatment. The middle red line for each plot is the median. The lower red line is the 25th percentile and the higher red line is the 75th percentile. Extreme data points are highlighted as whiskers extend outwards.*

Indentation hardness methods may yield different trends at various length scales [53]. In this study, Rockwell hardness was chosen because it is correlated with plastic deformation of the surface and it measures the hardness of a material as a response to the penetration depth of indentation [53]. Microhardness Vickers testing allows for the local surface hardness to be identified due to the lower applied load range when indenting the surface [53, 54]. Rockwell hardness and Vickers microhardness are both useful for understanding the significance of laboratory UV exposure and freeze-thaw cycling on the degradation of polystyrene.

Few studies examine the changes in plastic hardness as a result of environmental weathering. Budin and Jaafar studied the effects of natural outdoor weathering and salt water exposure (in a controlled laboratory setting) for 150 days on polylactic acid samples [55]. A decrease in macrohardness from Rockwell R hardness measurements was continuously observed over 30 day sampling intervals for both treatments [55]. Degradation of the polymer was primarily attributed to hydrolysis [55]. In contrast, Beltrán et al. immersed polylactic acid in a buffered solution at 37 ^{o}C with interval sampling and conducted microhardness testing [51]. An increase in polymer microhardness was identified due to the embrittlement process from hydrolytic degradation, which resulted in decreased polymer chain length [55]. However, the different hardness length scales (macro and micro) and different weathering techniques complicate the comparison of the results. This highlights the importance of analyzing multiple hardness length scales when complex weathering processes are present either in the laboratory setting or the natural environment.

It should also be noted that these studies focused on polylactic acid polymers as opposed to polystyrene. However, both polymers have a carbon backbone and are more suspectable to photodegradation induced from UV irradiance. The breaking of polymer chains from UV exposure as well as mechanical pressures on polystyrene sheets (from freezing-and thawing ice crystallization) could cause changes in material crystallinity [54, 56-58]. UV irradiance exposure also results in the formation of free hydrogen radicals, leading to surface hardening and the formation of microcracks [58, 59]. According to Yousif and Haddad, the UV irradiance of polystyrene increases the material crystallinity and decreases the molecular weight [57]. Several studies have concluded the effects of UV irradiance exposure utilizing additional characterization techniques such as Thermogravimetry Analyzer and Differential Scanning Calorimetry (determination of glass transition and degree of crystallinity), Gel Permeation Chromatography (molecular weight changes) and variations in oxidation [57, 58]. The increase in microhardness in this study when exposed to UV is consistent with increased crystallinity of the surface, and our results concur with other UV irradiance polystyrene weathering experimental findings in literature. Moreover, the observed reduction in microhardness upon exposure to FT and the effects of synergistic weathering (UV-FT) both highlight the relevance of simulating the southern Quebec natural environment in a laboratory setting.

3.3.2. Dynamic Mechanical Analysis of Modulus and Glass Transition Temperature

The weathering of plastics that leads to oxidation of the polymer chain will impact the material structure, causing it to be more brittle, and prone to irreversible deformation [49]. Dynamic Mechanical Analysis (DMA) characterization measures these viscoelastic properties [60]. A polymer's elastic response to shape recovery, as well as its viscous response to dispersing mechanical energy, is observed by measuring the modulus and glass transition temperature (T_g) [60]. A DMA temperature sweep is a sensitive test that can be utilized to determine polymer viscoelastic property changes within a thermally controlled environment, providing insight into polymer stiffness, and crystallinity. This test reports the modulus and damping effect on the material for transition temperatures as the heat is ramped up at a constant rate, enabling the Storage Modulus (*E'*), Loss Modulus (*E"*) and tan delta (*tan* δ) to be plotted as a function of temperature [61]. Changes in these properties give insight into the effect of weathering on the polymer matrix.

The mechanical energy stored within a material during the loading cycle of a DMA test can be measured using *E'* [60]. This parameter relates to polymer stiffness and shape recovery [60, 61]. Conversely, *E"* examines a material's damping behavior [60]. Internal molecular motions allow for mechanical energy to disperse throughout the polymer [61, 62]. Tan delta is a strong indicator of thermal-mechanical conditions that affect a material's bond rotation and intermolecular friction [60]. Equation 1 displays the relationship between *tan* δ, *E'* and *E"*.

$$\tan \delta = \frac{E''}{E'} \qquad eq. 1$$

Figure 4 (a, b, c) depicts representative curves obtained from a temperature sweep (6 ^{o}C/min, 1 Hz) for all polystyrene treatments. Table 1 displays the mean values of T_g for *E"*, *E'* and *tan* δ. Figure 4a illustrates significant changes in the storage modulus for UV+FT (89.77 ± 0.329 ^{o}C) and UV (89.64 ± 0.903 ^{o}C) treatments when compared to the control (86.24 ± 0.214 ^{o}C), unweathered (87.33 ± 0.212 ^{o}C) and FT (85.48 ± 0.930 ^{o}C). Although the mean T_g obtained from the *E'* curves for the control samples was not different from the unweathered and FT samples, this was not the case when comparing the latter two treatments. Unweathered and FT samples showed a significant difference when compared to one another as well as when compared to UV+FT and UV treatments.

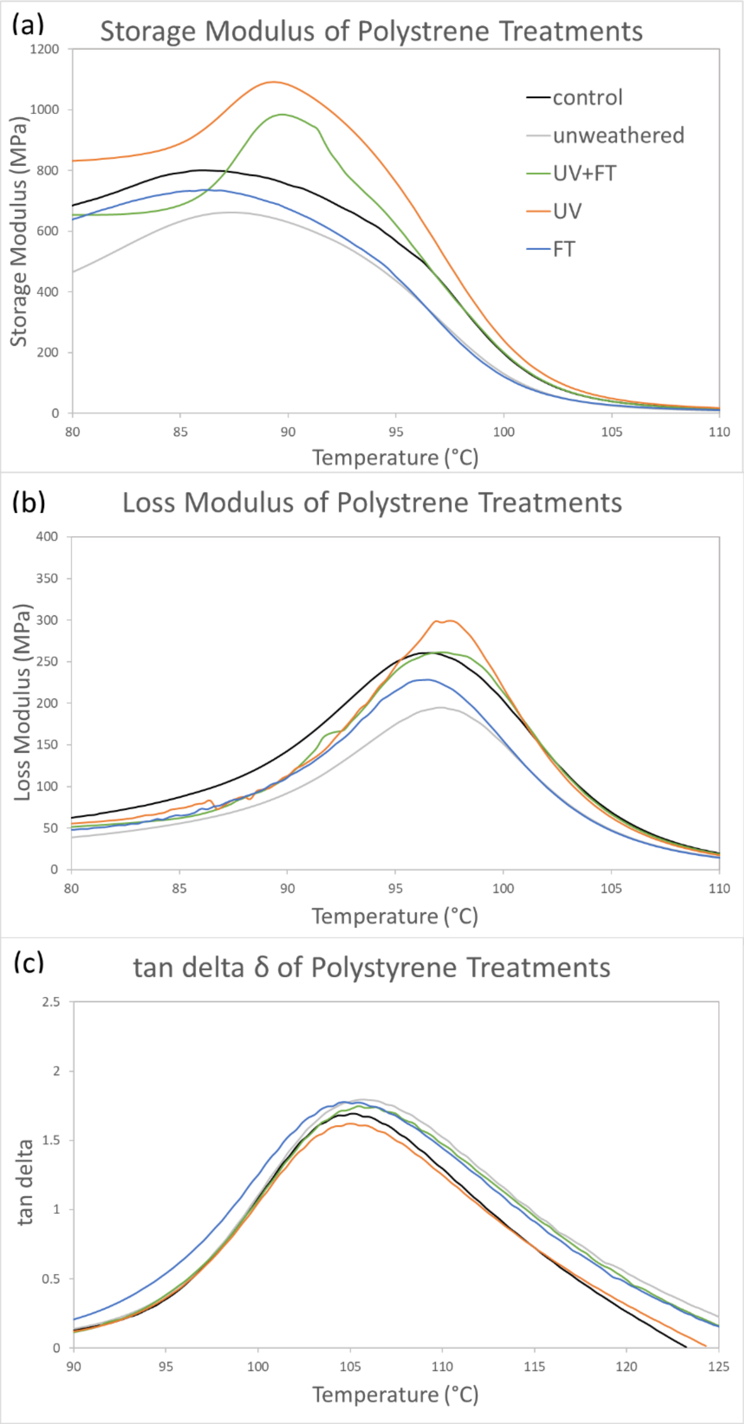

Figure 4. *Dynamic mechanical analysis measurements showing (a) Storage modulus as a function of temperature (b) Loss modulus as a function of temperature and (c) tan delta as a function of temperature. Representative curves were selected for each treatment. The selected curves indicate the closest absolute value of* T_g *to the mean whereby, N = 3 for each treatment.*

Table 1. Mean with Standard Deviation for T_g values obtained from *E”*, *E’* and *tan* δ.

	T_g (°C)		
Treatment	**loss modulus, *E”***	**storage modulus, *E’***	***tan δ***
control	97.0 ± 0.584	86.2 ± 0.214^{ab}	105 ± 0.295
unweathered	97.2 ± 0.374	87.3 ± 0.212^{a}	106 ± 0.278
UV+FT	97.5 ± 0.842	89.8 ± 0.329^{c}	106 ± 0.644
UV	97.6 ± 0.466	89.6 ± 0.903^{c}	105 ± 0.483
FT	96.4 ± 0.865	85.5 ± 0.930^{b}	105 ± 0.199

Note. Lettering denotes significance based on 1-way ANOVA test with post hoc Tukey’s HSD for each treatment ($p < 0.05$, n=3).

As polystyrene samples are heated, a phase transition takes place from elastic to fluid regimes as the polymer deforms [60]. The glass transition temperature is taken as the value when the viscous response dominates and deformation is determined to be irreversible [62]. The Q800 DMA software determines a T_g value from each *E’*, *E”* and *tan* δ curve. These values are unique for each parameter as they are a representation of a polymer’s different viscoelastic responses over a temperature range as opposed to at a single temperature [60]. Reported T_g values in literature are generally determined from the tan δ analysis as it tends to be more accurate, and best represents molecular motion within a polymer consistent with permanent deformation and rubbery flow [60, 62].

As expected, the reported T_g for *tan* δ (control 105 ± 0.295 ^{o}C) indicates a glass transition temperature that aligns with the material of polystyrene. Shinde et al. approximates a glass transition temperature for polystyrene to be 100 ^{o}C [63]. No significant differences were observed between treatments for *tan* δ. This illustrates that the identifiable composition of polystyrene remains intact for the various weathering treatments applied in this work. Bond rotation or intermolecular friction was not sufficiently impacted from weathering to affect the measured T_g of the bulk plastic. This implies that the effect of weathering may be more restricted to regions closer to the surface of the plastic.

The results obtained from the *E"* measurements further demonstrated there were no material composition changes. *E"* provides insight into a material's damping behavior, which enables a material to undergo molecular motions to disperse mechanical energy [60, 61]. A change in material composition (polymer chain scission, oxidation) that limits the damping behavior will induce a significant shift in the T_g curve. None of the reported T_g values for *E"* curves (Figure 4b) showed a significant change from the control (97.0 ± 0.584 ^{o}C).

Changes in a material's stored energy related to the shape recovery and stiffness are described by *E'* curves [61]. These mechanical properties of a material provide a better evaluation of weathering treatments on polystyrene. Significant changes were detected in the comparison of T_g for *E'* between the control and both UV and UV+FT treatments. A steeper drop in the *E'* curve from the peak indicates a rapidly decreasing modulus, which is a result of the material softening as it enters the rubbery flow region [60, 61, 64]. This can be seen in Figure 4a, whereby the UV and UV+FT treatments have steeper curves when compared to the more drawn out, gradual decrease observed for control, unweathered and FT. A more rigid polymer will have a higher T_g value, and a more flexible polymer will show a lower T_g value. The effects of UV and UV+FT led to a measurable increase in material stiffness as illustrated in the *E’* curves, which are shifted upward and to the right compared to control, unweathered and FT. This shift signals an increase in material crystallinity [61]. Polystyrene is an amorphous material, however, weathering leads to the formation of crystallites which allows it to behave as a two-phase system [65]. The crystalline phase will then inhibit the structural mobility of polystyrene amorphous regions, leading to changes in the storage modulus [65].

UV weathering was previously observed to decrease the molecular weight of polystyrene without evidence of crosslinking within the material structure [65]. This implies that mechanical property changes were attributed primarily to changes in hardness and material crystallinity [65]. Yousif and Haddid reported similar findings with UV-exposed samples of polystyrene [57]. The significant changes in T_g observed from *E’* in this study agree with the expected increase in both hardness and crystallinity from UV weathering. Our study shows that bulk polystyrene is undergoing mechanical property changes as expected when subjected to weathering. The shift in representative curves as well as significant changes in T_g for *E’* compliment the Rockwell hardness and Microhardness Vickers results. Both the Rockwell hardness and Microhardness Vickers increased for polystyrene samples exposed to UV and UV+FT when compared to control, unweathered and FT. Along with the observed increase in hardness, both at the macro and micro size ranges, UV and UV+FT treatments have shifted *E’* representative curves that are indicative of the formation of crystallites and a reduction in molecular weight (with no crosslinking mechanism) [57, 65].

In contrast to UV weathering, FT treatment was expected to make polystyrene less rigid and decrease its stiffness. When evaluating T_g values from the E' curves, FT was nor significantly different. This is in contrast to microhardness findings demonstrating a significant decrease in hardness for FT treatment.

3.3.2 Surface Roughness of Bulk Plastic Weathered Polystyrene

Surface changes of weathered bulk polystyrene samples can be examined in terms of surface roughness. It is important to quantify surface roughness because it highlights modifications to the outer layer of a material [66]. Structural and morphological differences can be detected and quantified [66]. Surface roughness measurements on polymers are frequently performed with Atomic Force Microscopy (AFM) [66-68]. This is a useful technique to observe the surface of a material at high resolution over a small area of significance. In this study, we used a Zygo interferometer profilometer, which is a 3D optical surfacing technique that produces a detailed image of the surface [68]. It is suitable for measuring surface roughness at high speed and with no material contact [68, 69]. A large area of the bulk polystyrene surface (1 inch x 1 inch) was scanned to obtain reliable quantitative data.

The surface roughness of a material can be measured using both height and functional parameters. S_a is defined as the arithmetical mean height. It is taken as the absolute value, expressed as the difference in height relative to the mean of the surface. Equation 2 displays how the Zygo profilometer determines the height parameter of S_a mathematically.

$$S_a = \frac{1}{A}\iint |Z(x,y)|dxdy \qquad eq. 2$$

A is the area of the mean plane, Z is the vertical plane (height parameter), x and y correspond to the coordinates on the x-plane and y-plane, respectively. S_a is a useful height parameter that identifies the average surface mean roughness.

S_{pk} is a functional parameter referred to as the reduced peak height of a materials surface [68, 70]. It accounts for the mean height of peaks above the core surface of a sample. Equation 3 illustrates how the S_{pk} value is calculated.

$$S_{pk} = \frac{2 \cdot A}{S_{mr1}} \qquad eq. 3$$

S_{mr1} is the bearing ratio which is obtained by the Mx Zygo software. According to Sorgato et al., the functional parameter S_{pk} is useful to characterize mechanical and frictional interactions occurring at the surface of a polymer interface [70]. If there is a high presence of protruding peaks from the core mean surface, this is an indication of a surface's wear resistance [71]. Therefore, it is of interest to evaluate S_{pk} values when polystyrene is exposed to photodegradation and freezing-thawing processes.

Zygo surface roughness measurements were evaluated at two magnifications (2.75x and 100x). These magnifications yielded the same trends regarding significant changes of the surface layer. This confirmed that S_a and S_{pk} values remained consistent when examining the surface of the samples at different distances.

Figure 5 illustrates the results of S_a and S_{pk} for all treatments. No significant differences were detected for S_a both at 2.75x (control 0.42 ± 0.06 um; unweathered 0.77 ± 0.31 um; UV+FT 1.02 ± 0.44 um; UV 0.41 ± 0.02 um; FT 0.62 ± 0.17 um) and 100x (control 0.21 ± 0.03 um; unweathered 0.36 ± 0.18 um; UV+FT 0.45 ± 0.15 um; UV 0.23 ± 0.08 um; FT 0.32 ± 0.12 um) for all treatments when compared to the control treatment. This demonstrates that average surface roughness (in terms of evaluating a surface height parameter) did not change when samples were subjected to weathering.

The functional parameter of S_{pk} exhibited a significant change in surface roughness for UV+FT both at 2.75x (1.75 ± 0.38 um) and 100x (1.15 ± 0.27 um) magnifications when compared to the control treatment. No significant changes were detected for all other treatments at 2.75x (control 0.62 ± 0.04 um; unweathered 1.03 ± 0.42 um; UV 0.62 ± 0.02 um; FT 0.92 ± 0.13 um) and 100x (control 0.40 ± 0.07 um; unweathered 0.44 ± 0.07 um; UV 0.46 ± 0.12 um; FT 0.47 ± 0.13 um) when compared to the control.

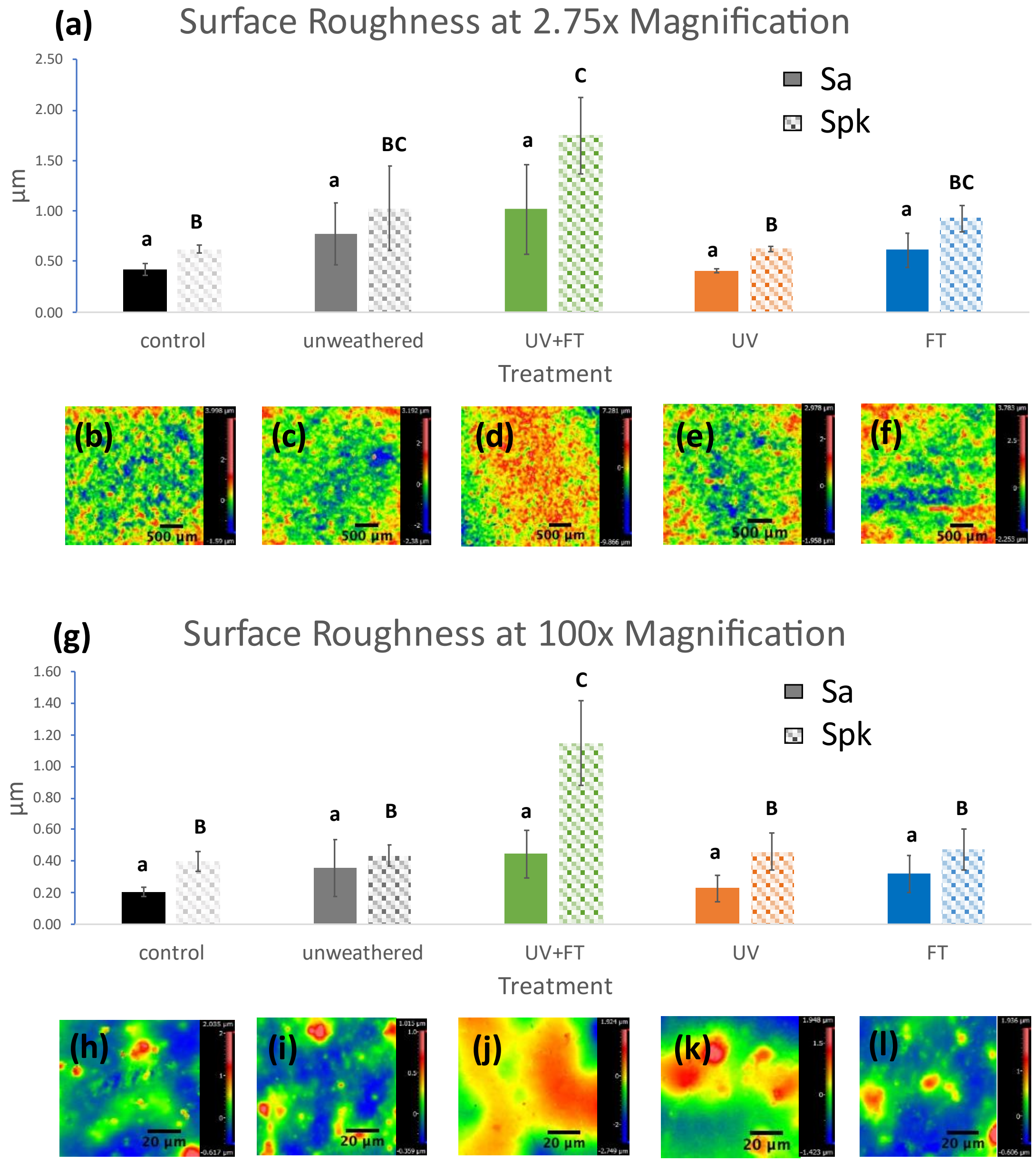

Figure 5. *(a) Sa and Spk values at 2.75x magnification. (b-f) Representative 2D profiles at 2.75x of control, unweathered, UV+FT, UV and FT, respectively. (g) Sa and Spk values at 100x magnification. (h-l) Representative 2D profiles at 100x of control, unweathered, UV+FT, UV and FT, respectively. *Note: All tests were performed N = 3 for each treatment and magnification. Lettering denotes significance of 1-way ANOVA test performed with post hoc Tukey's HSD ($p < 0.05$). Stats are compared to the same surface roughness parameter of Sa (lowercase) or Spk (uppercase), not to each other.*

Representative 3D surface profiles are depicted in Figure 6. It is clear that the 3D profiles exhibit a greater amount of elevated surface for UV+FT when compared to control. Red and orange colors indicate a raised profile. Blue is indicative of lower height (relative to the core surface) and topography of valleys on the surface of the material. Each representative 3D profile has a different scale relative to the core surface (depicted as zero) which is determined by Zygo (for the specified area of interest). For example, in Figure 6a (control 2.75x) the scale of peaks and valleys in the Z-direction is between 3.99 um and -1.59 um. Conversely, in Figure 6b (UV-FT 2.75x) the scale of peaks and valleys is from 7.28 um to -9.87 um. A similar conclusion can be drawn when examining the scales in the profiles at 100x (Figure 6c, d). This highlights the significant difference between control and UV+FT in terms of the formation of peaks and valleys relative to the core surface.

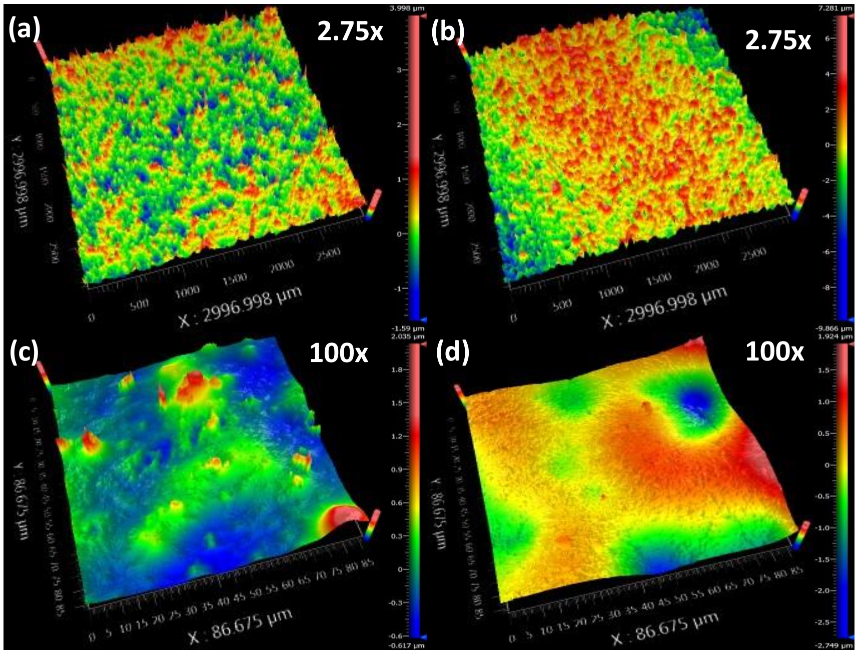

***Figure 6**. Representative 3D Zygo interferometer profiles of (a) control at 2.75x (b) UV+FT at 2.75x (c) control at 100x (d) UV+FT at 100x. Note: each image possesses a different scale as it is determined for the area of interest depicted.*

Due to the polymeric nature, as well as the mechanical-structural properties of polystyrene, it can be expected that weathering will induce surface layer changes. This was evident in evaluating the surface roughness results of S_{pk}. Rowenczyk et al. evaluated the surface roughness of weathered polyethylene samples from the ocean using AFM [66]. It was found that the root mean square (RMS) of roughness increased by a factor of two when compared to unweathered samples, indicating that weathering induced micro-sized peaks at a scale typical of semi-crystalline arrangement [66, 67]. Rowenczyk et al. highlight that embrittlement, fragmentation and morphological changes occur on the surface layer of weathered polyethylene and that similar effects may be observed for other polymers [66]. Non-homogeneous erosion of the surface layer due to processes such as oxidation and hydrolysis lead to a higher carbonyl index [66].

The synergistic effects of UV-FT weathering in our study clearly show an increased affinity for finer peak formation. Sorgato et al. determined that a higher presence of finer peaks is correlated to an increase in material roughness [70]. Our results obtained for the S_{pk} parameter of surface roughness align with this conclusion. However, it's not necessarily the peaks on the surface of UV+FT samples that increased in size and height, but rather erosion took place in-between peaks. This enabled the further protrusion of peaks relative to the core surface as particle fractionation most likely occurred. The S_{pk} parameter can also provide insight about surface wearability [71]. If a material is subjected to more wear and tear, it will exhibit a higher S_{pk} value [71]. This was observed in our study as the synergistic effects of UV+FT induced morphological changes on the surface.

The treatment of UV+FT underwent an increase in both Rockwell hardness and microhardness. These mechanical properties are associated with surface layer interactions and thus, combined with the increase in T_g and S_{pk}, it can be determined that synergistic processes are causing changes to mechanical properties and surface morphology. Huang et al. measured the surface roughness of polystyrene on a silica substrate to illustrate that an increase in T_g is associated with an increase in roughness [68]. These findings agree with both the dynamic mechanical analysis and the evaluation of surface roughness changes for synergistic weathering on bulk polystyrene in a simulated southern Quebec region.

3.3.4 SEM Morphology and NTA Concentration of Leachate Particles

Physical characterization of particles in the leachate was performed with scanning electron microscopy (SEM) and nanoparticle tracking analysis (NTA). When combined, these techniques provide a complementary approach that enables particle sizing, concentration, and morphology observations [72, 73]. Sizing information extracted from SEM gives direct visual representations of particle morphologies in addition to NTA which relies on light scattering (from the Brownian motion of individual particles) to determine particle concentrations for particles ranging from approximately 10 nm to 1 µm [43, 72, 74]. The quantification of sub-micron particles is important because it provides insight about the fractionation processes that may be occurring on the surface of the polystyrene coupons.

SEM images of the leachates are depicted in Figure 7 for UV+FT and FT treatments. Particles were observed at both low and high magnifications. Additional image analysis is needed to quantify the particle size distributions from the SEM images [72]. However, particles of a few hundred nanometers were observed consistently in SEM. The weathering of polystyrene led to the formation of particles with irregular morphologies and a high degree of polydispersity.

Figure 8 shows that the fridge control and procedural blank samples did not contain many visible particles, confirming that there was no substantial contamination from sample preparation and handling.

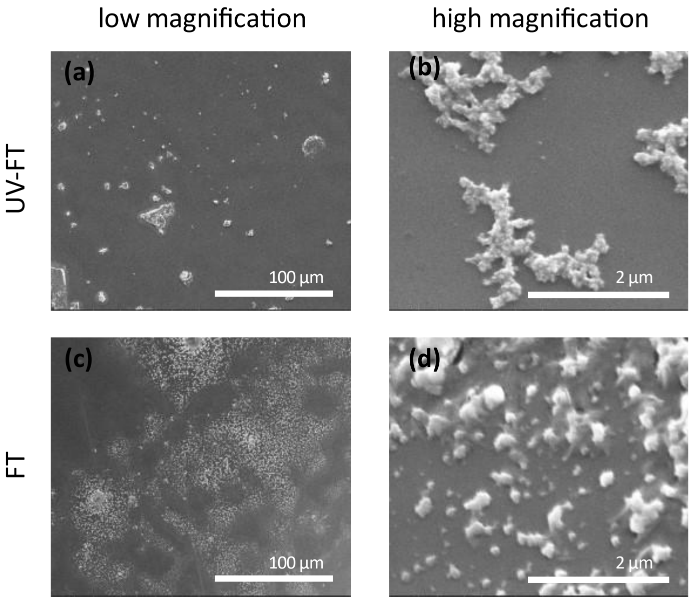

Figure 7. *SEM images of the leachates of polystyrene exposed to UV-FT or FT weathering. (a, c) Imaging at low magnification. (b, d) Imaging at high magnification.*

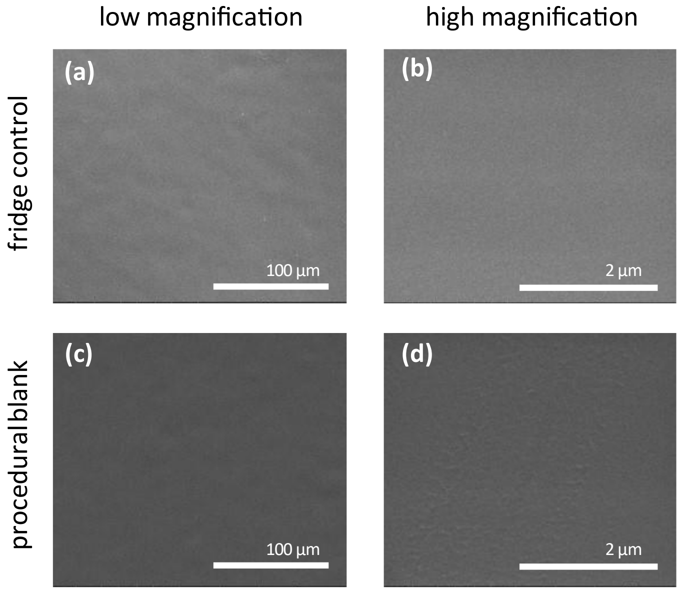

Figure 8. *SEM images of the fridge control and procedural blank. (a, c) Imaging at low magnification. (b, d) Imaging at high magnification.*

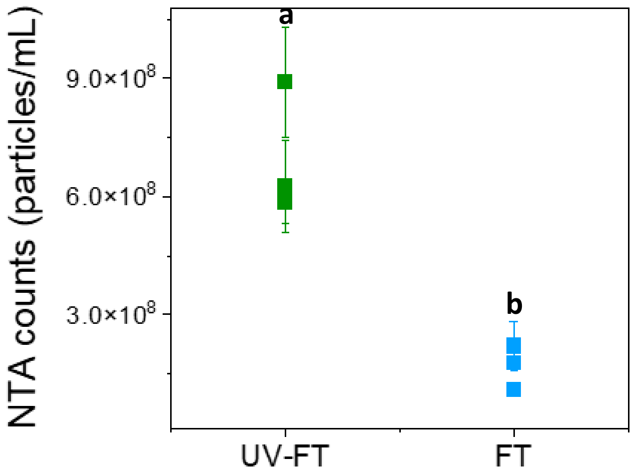

Figure 9. *NTA measurements of the leachates after UV-FT and FT treatments. Results were obtained by measuring three times each triplicate and tracking more than 200 particles per measurement (total of 9 measurements per weathering treatment). These tracks were then processed using the NanoSight software. Lettering indicates significance of 1-way ANOVA test performed with post hoc Tukey's HSD (p < 0.05).*

Table 2.

Mean with standard deviation for NTA particle counts (particles/mL) of Leachates. Particle sizes in the count range from ~ 10 nm to ~ 1 µm.

Treatment	**Particle Counts (particles/mL)**
control (fridge)	BDL
procedural blank	BDL
UV+FT	$7.02 \pm 1.85 \times 10^{8}$ **a**
FT	$1.69 \pm 0.62 \times 10^{8}$ **b**

Note. 1-way ANOVA test with post hoc Tukey's HSD for each treatment ($p < 0.05$, n=9). BDL = Below detection limit. Particle concentration was too low for NTA instrument. Letters indicate significance detected.

Nanoparticle tracking analysis results are illustrated in Figure 9. Mean particle count data is displayed in Table 2. It was determined that both UV-FT (7.02 ± 1.85 x 10^8 particles/mL) and FT (1.69 ± 0.62 x 10^8 particles/mL) leachates had particle concentrations on the order of 10^8 particles per mL. The combined synergistic weathering effects of UV+FT caused the release of significantly more particles when compared to FT weathering alone.

Both the fridge control and the procedural blank did not yield more than 100 tracks per measurement in NTA. Thus, the concentration of particles could not be determined, as it was most likely below the detection limit of the instrument. These findings are supported by the SEM images shown in Figure 8, where few particles were observed.

This study has emphasized the effects of weathering on polystyrene by examining both the bulk plastic samples as well as the leachate. The observations of particle release from SEM imaging depicts sizes within the micron and sub-micron ranges as expected. Size and shape observations of the particles exhibit non-uniform morphology, aggregate formation and polydispersity. This implies fragmentation occurring on the surface layer of polystyrene whereby, different particle sizes and morphologies are released into the leachate [66]. Moreover, the significant number of particles detected by NTA from synergistic UV-FT weathering suggest that combined mechanisms of degradation erode the surface layer of polystyrene. These findings agree with Rowenczyk et al. in that bulk polystyrene samples most likely underwent a combination of embrittlement from UV exposure, hydrolysis, oxidation, and an increase in surface roughness [66]. We have shown the number of particles released from the surface region of polystyrene during our experiments can be quantified at a magnitude of approximately 10^8 particles/mL. Lambert and Wagner confirmed that polystyrene forms nanoplastics when degraded in aquatic environments [43]. After 56 days of weathering, their study identified a concentration of 1.26 x 10^8 particles/mL of polystyrene nanoplastics [43]. We recorded a similar magnitude (10^8) of particles detected with the same technique of NTA. Our study also integrated synergistic weathering with UV-FT and only FT. Lambert and Wagner used UV exposure (320-400 nm) for their experiment.[53] A study conducted by Song et al. measured approximately 3.6 ± 1.3 x 10^8 and 5.6 ± 2.9 x 10^8 particles/cm^2 after 12 and 24 months respectively, for the outdoor weathering of expanded polystyrene [75]. This shows that our simulated laboratory weathering is on par with the range of particles released, even in an outdoor setting.

3.3.5 Characterization of Leachate Particle Chemical Composition

Fourier transform infrared spectroscopy is a characterization technique that is commonly used to identify the chemical composition of polymers [76]. However, it is challenging to identify low concentrations of small particles unless they are analyzed as films or agglomerates [38]. Bulk polystyrene coupons were compared to films composed of micron-sized and sub-micron sized particles from the leachate to confirm matching spectra. This allowed for the identification of polystyrene polymer functional groups as well as chemical changes to the weathered bulk coupon surface (i.e. oxidation).

Figure 10a-c and Figure 11 present the FTIR measurements for treatments relative to unweathered bulk polystyrene plastic. The micron and submicron films displayed in UV-FT (Fig. 10b) and FT (Fig. 10c), yielded low signals that are likely the result of the relatively low mass of material deposited on the substrate. However, it was still possible to identify the major characteristic peaks of polystyrene. For all micron-sized and sub-micron sized particle films, peaks were detected at 2825-3100 cm^{-1} ($-CH_2$ and aromatic -CH stretches, multiple peaks), 1450-1500 cm^{-1} ($-CH_2$ bend and aromatic ring stretch, two peaks), 750-760 cm^{-1} (ring in-phase H wag, one peak), 695-700 cm^{-1} (aromatic CH out-of-plane bend, one peak) and 535-540 cm^{-1} (aromatic ring out-of-plane bend, one peak). These peaks were also detected in the unweathered and treated bulk plastic. Thus, it can be concluded that polystyrene samples released polystyrene particles to the leachate after being exposed to UV-FT and FT treatments.

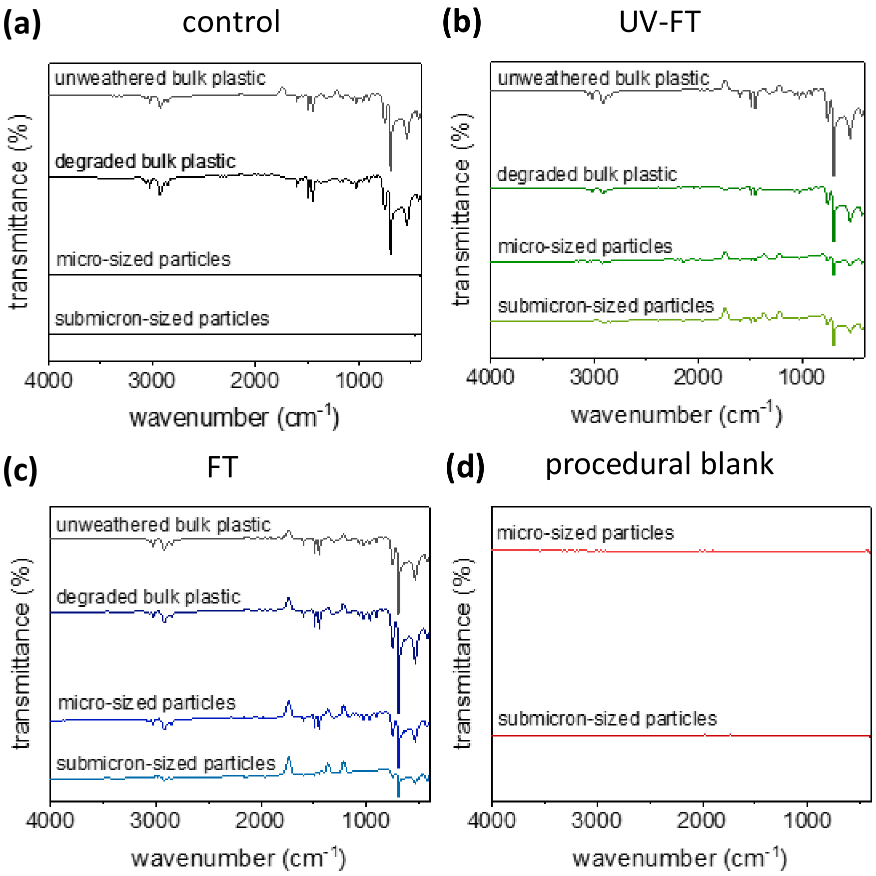

Figure 10. *FTIR spectra for (a) control bulk plastics before and after fridge weathering and their corresponding micro and submicron films, (b) UV-FT treatment bulk plastics before and after weathering and their corresponding micron and submicron films, (c) FT treatment bulk plastics before and after weathering and their corresponding micron and submicron films, and (d) the micron and submicron films of the procedural blank.*

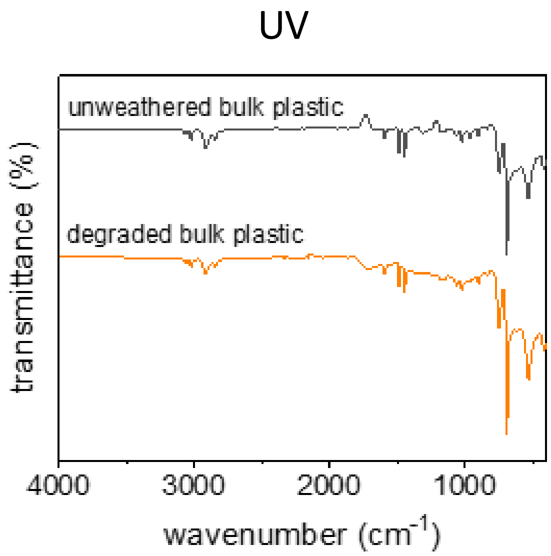

Figure 11. *UV-only treatment of bulk plastic before and after weathering.*

Figure 11 shows differences in the carbonyl groups (-C=O) (1600-1800 cm^{-1}) between UV-degraded and unweathered polystyrene. The peak confirms oxidation taking place on the outermost layer of the plastic. As expected, this carbonyl group change is seen in UV-FT (Figure 10b) when comparing the unweathered bulk plastic to the degraded bulk plastic. Both the fridge control (Fig. 10a) and procedural blank (Fig. 10d) yielded no films when the leachates were drop-casted. This was confirmed with FTIR as no signal was detected. These results further corroborate the SEM and NTA findings for the fridge control and procedural control. Very few particles were detected and quantified; thus, it was expected that we would be unable to form films from the leachate that could be analyzed by FTIR.

The results corroborate several studies in that FTIR is a suitable test to identify chemical composition for films of micron-sized and submicron-sized polystyrene particles [38, 77, 78]. Our findings also coincide with weathered bulk plastic spectra for polystyrene outdoor and indoor weathering experiments [64, 79].

3.4 Conclusions

This study has demonstrated that simulating the southern Quebec region (within the laboratory setting) weathering conditions on polystyrene, namely synergistic UV-FT, led to changes in mechanical properties and surface roughness. The effects of weathering were further investigated to identify micron-sized and submicron-sized polystyrene particles released in the leachate. For UV-FT treatments, both Rockwell hardness and microhardness measurements indicated an increase in macro- and micro-hardness, respectively. This was attributed to the synergistic effects of UV followed by FT, ultimately causing bulk polystyrene to become brittle and degraded on the surface layer. An analysis of the *E'* curves illustrated a shift in T_g concurrent with increased crystallite formation and increased polymer stiffness/embrittlement. No apparent changes were observed for the *E"* or *tan* δ curves, indicating that the damping behavior and the bond rotation (i.e. intermolecular friction) of polystyrene remained intact. This is important as FTIR confirmed functional group fingerprint identification of peaks showing that all weathered bulk samples were a chemical composition match for polystyrene at the surface level. The surface roughness was then evaluated with the height parameter, S_a and the functional parameter, S_{pk}. It was found that no changes occurred to S_a indicating that the absolute value of the peaks and valleys, relative to the mean surface, did not change. However, further analysis of the S_{pk} values illustrated that synergistic UV-FT did indeed cause a significant increase in reduced peak height relative to the core of the surface. This affirms that surface peaks became finer as synergistic weathering enabled erosion to take place at the core surface. With increased finer peaks relative to the core, this infers the peaks themselves do not grow in height. Lastly, both SEM and NTA revealed the release of particles in the leachate that were identified as polystyrene in FTIR. A larger number of particles were released for synergistic UV-FT when compared to FT alone. However, treatments of UV-FT and FT both showed unique particle morphologies, irregular size and shapes along with polydispersity. Very few particles were released in the control and procedural blank within the micron and submicron sizes, further highlighting the benefits of simulated laboratory weathering with no substantial contamination. Our findings align with literature results and provide further insight when evaluating the environmental concerns associated with weathering and particle release of polystyrene in a climate like southern Quebec where several seasons are present.

4 Conclusions and Future Work

Weathering and degradation pathways leading to potential fragmentation (potentially due to embrittlement from oxidation, change in stiffness, and surface roughness) of particles from the surface layer were illustrated by characterizing bulk polystyrene. We showed that synergistic weathering, particularly with the inclusion of FT in a closed system needs to be further investigated. More polymers need to be evaluated in FT conditions. Polystyrene has a carbon backbone and therefore, our results provide some insight as to how other polymers with a similar structure may behave (i.e. polypropylene, high density polyethylene, and low density polypropylene) when subjected to similar climate conditions. Although our findings detected concentrations of micron-sized and submicron-sized particles similar to weathering experiments conducted with other polymers in an outdoor setting (~10^8 particles/mL), it would add more clarity to the findings if an experiment was conducted in unison with outdoor weathering in the region of interest. This would allow for a direct comparison to be made. There is a need for a protocol and harmonization when conducting future FT experiments. Many regions around the world experience climates that undergo cyclical UV irradiation and/or freeze-thaw. Hence, our study is positioned well to highlight the importance of better understanding the effects of FT on plastic degradation and particle release.

The characterization of polymer mechanical properties is a diverse field. There are several critical reviews and techniques to choose from to determine physical property changes. Our study focused on hardness at the macro and micro levels as well as dynamic mechanical analysis. There were no major changes in measurements of UV-FT hardness at the different length scales. However, it would be interesting to further analyze the hardness with a nano-indenter. This would allow for an in-depth comprehensive assessment of hardness at all the major length scales even though our UV-FT results clearly depict an increase in hardness for polystyrene due to degradation as expected. Perhaps nano-indentation would provide even more insight for particle fragmentation. It would also be useful to conduct Thermogravimetric Analysis or Differential Scanning Calorimetry experiments to determine T_g, and molecular weight. These tests could further corroborate our findings for surface roughness, hardness and Elastic Modulus. A comprehensive analysis would be obtained for oxidation, embrittlement and crystallite formation in the polymer matrix. This is important because there is a relationship between molecular weight, crystallinity, and glass transition temperature. Molecular weight decreases with an increase in crystallite formation and a polymer may become more brittle due to oxidation. We found that our results came to the same conclusion as these relationships and the subsequent effects on polystyrene are well documented.

Further SEM analysis of the weathered bulk polystyrene would allow for surface bulk morphology observation. It would be expected that we would observe cracks and flakes on the surface. These findings would coincide with the effects of oxidation and provide further understanding of fragmentation of the surface layer as particles are released.

The environmental implications of synergistic weathering that includes FT will have to be examined more closely as the formation and occurrence of microplastics and nanoplastics continues to be a global issue. Our research is applicable to many climates around the world that could have similar effects on the weathering of plastics.

Bibliography

1. Borrelle, S.B., et al., *Predicted growth in plastic waste exceeds efforts to mitigate plastic pollution.* Science, 2020. **369**(6509): p. 1515-1518.
2. Alimi, O.S., et al., *Weathering pathways and protocols for environmentally relevant microplastics and nanoplastics: What are we missing?* Journal of Hazardous Materials, 2022. **423**: p. 126955.
3. Carbery, M., W. O'Connor, and T. Palanisami, *Trophic transfer of microplastics and mixed contaminants in the marine food web and implications for human health.* Environment International, 2018. **115**: p. 400-409.
4. Gigault, J., et al., *Nanoplastics are neither microplastics nor engineered nanoparticles.* Nature Nanotechnology, 2021. **16**(5): p. 501-507.
5. Jeong, C.B., et al., *Adverse effects of microplastics and oxidative stress-induced MAPK/Nrf2 pathway-mediated defense mechanisms in the marine copepod Paracyclopina nana.* Scientific Reports, 2017. **7**.
6. Alimi, O.S., et al., *Microplastics and Nanoplastics in Aquatic Environments: Aggregation, Deposition, and Enhanced Contaminant Transport.* Environmental Science & Technology, 2018. **52**(4): p. 1704-1724.
7. Bouwmeester, H., P.C.H. Hollman, and R.J.B. Peters, *Potential Health Impact of Environmentally Released Micro- and Nanoplastics in the Human Food Production Chain: Experiences from Nanotoxicology.* Environmental Science & Technology, 2015. **49**(15): p. 8932-8947.
8. Della Torre, C., et al., *Accumulation and Embryotoxicity of Polystyrene Nanoparticles at Early Stage of Development of Sea Urchin Embryos Paracentrotus lividus.* Environmental Science & Technology, 2014. **48**(20): p. 12302-12311.
9. Besseling, E., et al., *Nanoplastic Affects Growth of S. obliquus and Reproduction of D. magna.* Environmental Science & Technology, 2014. **48**(20): p. 12336-12343.
10. Bergami, E., et al., *Nano-sized polystyrene affects feeding, behavior and physiology of brine shrimp Artemia franciscana larvae.* Ecotoxicology and Environmental Safety, 2016. **123**: p. 18-25.
11. Canesi, L., et al., *Interactions of cationic polystyrene nanoparticles with marine bivalve hemocytes in a physiological environment: Role of soluble hemolymph proteins.* Environmental Research, 2016. **150**: p. 73-81.
12. Casado, M.P., A. Macken, and H.J. Byrne, *Ecotoxicological assessment of silica and polystyrene nanoparticles assessed by a multitrophic test battery.* Environment International, 2013. **51**: p. 97-105.
13. Cedervall, T., et al., *Food Chain Transport of Nanoparticles Affects Behaviour and Fat Metabolism in Fish.* PLOS ONE, 2012. **7**(2): p. e32254.
14. Cole, M. and T.S. Galloway, *Ingestion of Nanoplastics and Microplastics by Pacific Oyster Larvae.* Environmental Science & Technology, 2015. **49**(24): p. 14625-14632.
15. Crater, J.S. and R.L. Carrier, *Barrier Properties of Gastrointestinal Mucus to Nanoparticle Transport.* Macromolecular Bioscience, 2010. **10**(12): p. 1473-1483.

16. Greven, A.C., et al., *Polycarbonate and polystyrene nanoplastic particles act as stressors to the innate immune system of fathead minnow (Pimephales promelas).* Environ Toxicol Chem, 2016. **35**(12): p. 3093-3100.
17. Mattsson, K., et al., *Altered Behavior, Physiology, and Metabolism in Fish Exposed to Polystyrene Nanoparticles.* Environmental Science & Technology, 2015. **49**(1): p. 553-561.
18. Sarno, A., et al., *Accelerated Hydrolysis Method for Producing Partially Degraded Polyester Microplastic Fiber Reference Materials.* Environmental Science & Technology Letters, 2021. **8**(3): p. 250-255.
19. Cai, L., et al., *Observation of the degradation of three types of plastic pellets exposed to UV irradiation in three different environments.* Science of The Total Environment, 2018. **628-629**: p. 740-747.
20. Bianchetti, G.O., C.L. Devlin, and K.R. Seddon, *Bleaching systems in domestic laundry detergents: a review.* RSC Advances, 2015. **5**(80): p. 65365-65384.
21. Lapointe, M., et al., *Understanding and Improving Microplastic Removal during Water Treatment: Impact of Coagulation and Flocculation.* Environmental Science & Technology, 2020. **54**(14): p. 8719-8727.
22. Sahan, M., *The measurements of the global solar radiation and solar ultraviolet radiation during 2018 year.* AIP Conference Proceedings, 2019. **2178**(1): p. 030016.
23. Alimi, O.S., J.M. Farner, and N. Tufenkji, *Exposure of nanoplastics to freeze-thaw leads to aggregation and reduced transport in model groundwater environments.* Water Research, 2021. **189**: p. 116533.
24. Hakimzadeh, A., et al., *Exposure to Freeze–Thaw Conditions Increases Virulence of Pseudomonas aeruginosa to Drosophila melanogaster.* Environmental Science & Technology, 2018. **52**(24): p. 14180-14186.
25. Kingsbury, C.M. and T.R. Moore, *The Freeze-Thaw Cycle of A Subarctic Fen, Northern Quebec, Canada.* Arctic and Alpine Research, 1987. **19**(3): p. 289-295.
26. Asadishad, B., S. Ghoshal, and N. Tufenkji, *Role of Cold Climate and Freeze–Thaw on the Survival, Transport, and Virulence of Yersinia enterocolitica.* Environmental Science & Technology, 2013. **47**(24): p. 14169-14177.
27. Asadishad, B., et al., *Transport, motility, biofilm forming potential and survival of Bacillus subtilis exposed to cold temperature and freeze–thaw.* Water Research, 2014. **58**: p. 239-247.
28. Zaidi, L., et al., *Effect of natural weather on the structure and properties of polylactide/Cloisite 30B nanocomposites.* Polymer Degradation and Stability, 2010. **95**(9): p. 1751-1758.
29. Andrady, A.L., *Microplastics in the marine environment.* Marine Pollution Bulletin, 2011. **62**(8): p. 1596-1605.
30. Shah, A.A., et al., *Biological degradation of plastics: A comprehensive review.* Biotechnology Advances, 2008. **26**(3): p. 246-265.
31. Gewert, B., M.M. Plassmann, and M. MacLeod, *Pathways for degradation of plastic polymers floating in the marine environment.* Environmental Science: Processes & Impacts, 2015. **17**(9): p. 1513-1521.

32. Shah, S.S., I. Ahmad, and M. Ishaq, *Degradation study of used polystyrene with UV irradiation.* Advanced Materials Science, 2017. **2**: p. 1-6.
33. Adhikary, K.B., S. Pang, and M.P. Staiger, *Effects of the accelerated freeze-thaw cycling on physical and mechanical properties of wood flour-recycled thermoplastic composites.* Polymer Composites, 2010. **31**(2): p. 185-194.
34. Niu, F., et al., *Performance degradation of polymer material under freeze-thaw cycles: A case study of extruded polystyrene board.* Polymer Testing, 2021. **96**: p. 107067.
35. Farner, J.M., et al., *Effect of freeze/thaw on aggregation and transport of nano-TiO2 in saturated porous media.* Environmental Science: Nano, 2020. **7**(6): p. 1781-1793.
36. Wright, S.L. and F.J. Kelly, *Plastic and Human Health: A Micro Issue?* Environmental Science & Technology, 2017. **51**(12): p. 6634-6647.
37. Jambeck, J.R., et al., *Plastic waste inputs from land into the ocean.* Science, 2015. **347**(6223): p. 768-771.
38. Hernandez, L.M., N. Yousefi, and N. Tufenkji, *Are There Nanoplastics in Your Personal Care Products?* Environmental Science & Technology Letters, 2017. **4**(7): p. 280-285.
39. Besseling, E., et al., *Fate of nano- and microplastic in freshwater systems: A modeling study.* Environmental Pollution, 2017. **220**: p. 540-548.
40. Gigault, J., et al., *Marine plastic litter: the unanalyzed nano-fraction.* Environmental Science: Nano, 2016. **3**(2): p. 346-350.
41. Mattsson, K., et al., *Chapter 13 - Nanoplastics in the Aquatic Environment*, in *Microplastic Contamination in Aquatic Environments*, E.Y. Zeng, Editor. 2018, Elsevier. p. 379-399.
42. Jakubowicz, I., J. Enebro, and N. Yarahmadi, *Challenges in the search for nanoplastics in the environment—A critical review from the polymer science perspective.* Polymer Testing, 2021. **93**: p. 106953.
43. Lambert, S. and M. Wagner, *Characterisation of nanoplastics during the degradation of polystyrene.* Chemosphere, 2016. **145**: p. 265-268.
44. Kik, K., B. Bukowska, and P. Sicińska, *Polystyrene nanoparticles: Sources, occurrence in the environment, distribution in tissues, accumulation and toxicity to various organisms.* Environmental Pollution, 2020. **262**: p. 114297.
45. Erni-Cassola, G., et al., *Distribution of plastic polymer types in the marine environment; A meta-analysis.* Journal of Hazardous Materials, 2019. **369**: p. 691-698.
46. Mataji, A., M.S. Taleshi, and E. Balimoghaddas, *Distribution and Characterization of Microplastics in Surface Waters and the Southern Caspian Sea Coasts Sediments.* Archives of Environmental Contamination and Toxicology, 2020. **78**(1): p. 86-93.
47. Ward, C.P., et al., *Sunlight Converts Polystyrene to Carbon Dioxide and Dissolved Organic Carbon.* Environmental Science & Technology Letters, 2019. **6**(11): p. 669-674.
48. Azimzada, A., et al., *Single- and Multi-Element Quantification and Characterization of TiO2 Nanoparticles Released From Outdoor Stains and Paints.* Frontiers in Environmental Science, 2020. **8**(91).
49. Azimzada, A., et al., *Release of TiO2 nanoparticles from painted surfaces in cold climates: characterization using a high sensitivity single-particle ICP-MS.* Environmental Science: Nano, 2020. **7**(1): p. 139-148.

50. Siregar, J., et al., *The effect of alkali treatment on the mechanical properties of short pineapple leaf fibre (PALF) reinforced high impact polystyrene (HIPS) composites.* Journal of Food, Agriculture & Environment, 2010. **8**(2): p. 1103-1108.
51. Beltrán, F.R., et al., *Effect of different mechanical recycling processes on the hydrolytic degradation of poly(l-lactic acid).* Polymer Degradation and Stability, 2016. **133**: p. 339-348.
52. 785-98, A.S.D., *Standard Test Method for Rockwell Hardness of Plastics and Electrical Insulating Materials.* Annual Book of ASTM Standard, 2002. **8**.
53. Broitman, E., *Indentation Hardness Measurements at Macro-, Micro-, and Nanoscale: A Critical Overview.* Tribology Letters, 2016. **65**(1): p. 23.
54. Liu, X. and K. Hu, *Studies on photoprotection and photo-oxidation in polystyrene with various wavelength regions.* Polymers for Advanced Technologies, 1996. **7**(2): p. 117-121.
55. Budin, S. and M. Jaafar, *Comparative study on mechanical properties of virgin and recycled polylactic acid aging in natural weathering and seawater environment.* Polymer Bulletin, 2021.
56. Sousa, A.R., et al., *The combined effect of photodegradation and stress cracking in polystyrene.* Polymer Degradation and Stability, 2006. **91**(7): p. 1504-1512.
57. Yousif, E. and R. Haddad, *Photodegradation and photostabilization of polymers, especially polystyrene: review.* SpringerPlus, 2013. **2**(1): p. 398.
58. Castro Monsores, K.G.d., et al., *Influence of ultraviolet radiation on polystyrene.* Journal of Materials Research and Technology, 2021. **13**: p. 359-365.
59. Nishimori, F., et al., *Characterization of the surface degraded layer of polymers using an indentation method.* Materials Today Communications, 2021. **26**: p. 101873.
60. Dunson, D., *Characterization of polymers using dynamic mechanical analysis (DMA).* EAG Appl Note, 2017.
61. Worzakowska, M., *Thermal and mechanical properties of polystyrene modified with esters derivatives of 3-phenylprop-2-en-1-ol.* Journal of Thermal Analysis and Calorimetry, 2015. **121**(1): p. 235-243.
62. Poletto, M., M. Zeni, and A.J. Zattera, *Dynamic mechanical analysis of recycled polystyrene composites reinforced with wood flour.* Journal of applied polymer science, 2012. **125**(2): p. 935-942.
63. Remili, C., et al., *Photo-oxidation of polystyrene/clay nanocomposites under accelerated UV exposure: Effect on the structure and molecular weight.* Journal of Applied Polymer Science, 2009. **112**(5): p. 2868-2875.
64. Ainali, N.M., D.N. Bikiaris, and D.A. Lambropoulou, *Aging effects on low- and high-density polyethylene, polypropylene and polystyrene under UV irradiation: An insight into decomposition mechanism by Py-GC/MS for microplastic analysis.* Journal of Analytical and Applied Pyrolysis, 2021. **158**: p. 105207.
65. Shinde, V.V., et al., *Self-healing in high impact polystyrene (HIPS) composites via embedded non-toxic solvent-filled microcapsules.* Journal of Applied Polymer Science, 2022. **139**(2): p. 51463.
66. Rowenczyk, L., et al., *Microstructure Characterization of Oceanic Polyethylene Debris.* Environmental Science & Technology, 2020. **54**(7): p. 4102-4109.

67. Crist, B. and J.M. Schultz, *Polymer spherulites: A critical review.* Progress in Polymer Science, 2016. **56**: p. 1-63.
68. Huang, X., et al., *Experimental study of substrate roughness on the local glass transition of polystyrene.* The Journal of Chemical Physics, 2020. **152**(24): p. 244901.
69. Ghodrati, S., M. Mohseni, and S. Gorji Kandi, *Application of image edge detection methods for precise estimation of the standard surface roughness parameters: Polypropylene/ethylene-propylene-diene-monomer blend as a case study.* Measurement, 2019. **138**: p. 80-90.
70. Sorgato, M., D. Masato, and G. Lucchetta, *Tribological effects of mold surface coatings during ejection in micro injection molding.* Journal of Manufacturing Processes, 2018. **36**: p. 51-59.
71. Pawlus, P. and A. Dzierwa, *Tribological Behavior of Functional Surface: Models and Methods.* Coatings, 2021. **11**(3): p. 333.
72. Caputo, F., et al., *Measuring particle size distribution and mass concentration of nanoplastics and microplastics: addressing some analytical challenges in the sub-micron size range.* Journal of Colloid and Interface Science, 2021. **588**: p. 401-417.
73. Barbosa, F., et al., *A critical viewpoint on current issues, limitations, and future research needs on micro-and nanoplastic studies: From the detection to the toxicological assessment.* Environmental research, 2020. **182**: p. 109089.
74. Mintenig, S., et al., *Closing the gap between small and smaller: towards a framework to analyse nano-and microplastics in aqueous environmental samples.* Environmental Science: Nano, 2018. **5**(7): p. 1640-1649.
75. Song, Y.K., et al., *Rapid production of micro-and nanoplastics by fragmentation of expanded polystyrene exposed to sunlight.* Environmental Science & Technology, 2020. **54**(18): p. 11191-11200.
76. Silva, A.B., et al., *Microplastics in the environment: Challenges in analytical chemistry-A review.* Analytica chimica acta, 2018. **1017**: p. 1-19.
77. Ekvall, M.T., et al., *Nanoplastics formed during the mechanical breakdown of daily-use polystyrene products.* Nanoscale Advances, 2019. **1**(3): p. 1055-1061.
78. Mattsson, K., et al., *Nanofragmentation of expanded polystyrene under simulated environmental weathering (thermooxidative degradation and hydrodynamic turbulence).* Frontiers in Marine Science, 2021. **7**: p. 1252.
79. Shi, Y., et al., *Natural weathering severity of typical coastal environment on polystyrene: Experiment and modeling.* Polymer Testing, 2019. **76**: p. 138-145.